euronoise 2021
25th to 27th of October
Madeira, Portugal - online

Analytical solution for diffraction by finite edges in frequency domain

Petros Nikolaou[1], Penelope Menounou[1]

[1]Department of Mechanical Engineering and Aeronautics, University of Patras, Patras, Greece
(email: petros7nikolaou@gmail.com)

Abstract
An analytical solution for diffraction of spherical waves by finite edges in frequency domain is presented. As opposed to other analytical formulas, the presented solution does not require integration along the edge. The solution is composed of elementary functions and exponential integrals. The latter are well-studied and easy to compute analytic expressions. The accuracy of the presented solution is determined by comparisons with a well-established integral formula. Furthermore, based on the presented solution, specific criteria are developed which determine whether the infinite edge solution can be applied to a finite edge diffraction problem. These criteria are simple and can be used without calculating the finite edge solution.

Keywords: edge diffraction, analytical solution, finite edge, finite length

1 Introduction

Analytical solutions for diffraction by edges of finite length or simply finite edges exist in both frequency and time domain. In frequency domain the majority of analytical solutions have the form of a line integral along the diffracting edge [1]-[3]. To the best of the authors' knowledge the only solution in frequency domain that can be expressed as an analytic expression rather than an integral along the edge is the Ufimtsev solution [4] for the diffraction of a plane wave by the sides of a strip.

In the present work a frequency domain solution for the diffraction of spherical waves by finite edges is derived. The resulting formula contains elementary functions and exponential integrals which are well-studied analytic expressions. The solution derives from the Fourier integral of a time domain impulse response solution for the diffraction of spherical signals by finite edges [5]. It will be shown that, the presented solution converges to the solution for infinite edges of ref. [6] as the length of the edge increases. Furthermore, specific limits after which one can use the infinite edge solution of [6] instead of the presented finite edge solution for a problem of diffraction by a finite edge will be determined.

The time domain finite edge solution is presented in section 2. The derivation of the frequency domain finite edge solution is presented in section 3 and its accuracy is discussed in section 4. Finally, in section 5 limits after which one can use the infinite edge solution instead of the finite edge formula are determined.

2 Time Domain Solution

Consider a finite edge such as that of Figure 1 and a cylindrical frame of reference (r,ϕ,z). The source is located at $S(r_S,\phi_S,z_S)$ and the receiver at $R(r_R,\phi_R,z_R)$. The point Ξ in Figure 1 (b) and (c) defines the shortest path from the source to the edge line and from the edge line to the receiver $(S-\Xi-R)$. The point

Ξ is named reference point and the path $S-\Xi-R$ is named reference path. The length of the reference path is termed L, while the lengths of the paths through the edge ends $E_1(0,0,l_1)$ and $E_2(0,0,l_2)$ ($S-E_1-R$ and $S-E_2-R$), are termed L_1 and L_2, respectively. It is

$$\begin{aligned} L &= \sqrt{\left(r_R + r_S\right)^2 + \left(z_R - z_S\right)^2} \\ L_{1,2} &= \sqrt{\left(l_{1,2} - z_S\right)^2 + r_S^2} + \sqrt{\left(l_{1,2} - z_R\right)^2 + r_R^2} \end{aligned} \tag{1}$$

A time domain solution for the diffraction of spherical signals by finite edges has been presented in previous work of the authors [5]. The solution is

$$p_{irf,\,finite}^{d} = \pm\frac{1}{2}H\left(L_1/c - t\right)p_{irf}^{d}(t) + \frac{1}{2}H\left(L_2/c - t\right)p_{irf}^{d}(t), \tag{2}$$

where the positive sign in Eq. (2) is used in the case where the reference point lies within the edge ends [Figure 1 (b)] and the negative sign is used in the case where the reference point lies outside the edge ends [Figure 1 (c)]. The symbol H stands for the Heaviside function [$H(x)=0$ for $x<0$ and $H(x)=1$ for $x>1$], the symbol c is the speed of sound, and p_{irf}^{d} is the solution for infinite edges also found in ref. [5].

$$p_{irf}^{d} = p_{irf}^{di} + p_{irf}^{dr} = -\left[\sqrt{c}\Big/\left(2\pi\sqrt{L}\sqrt{r_R r_S}\right)\right]\cdot\left(\bar{t}_{di}\Phi_{di}\left[\sqrt{\tau}\left(\tau+\tau_{lag}^{di}\right)\right]^{-1} + \bar{t}_{dr}\Phi_{dr}\left[\sqrt{\tau}\left(\tau+\tau_{lag}^{dr}\right)\right]^{-1}\right), \tag{3}$$

where the component p_{irf}^{di} is associated with the incident signal and p_{irf}^{dr} is associated with the reflected signal by the side of the barrier facing the source [Figure 1 (a)]. The variable τ is defined as $\tau = t - L/c$ and expresses a time that starts to measure exactly when the diffracted signal by an infinite edge arrives to the receiver ($\tau = 0$ for $t = L/c$). The parameters $\bar{t}_{di,dr}$ are time parameters given by $\bar{t}_{di,dr} = r_S r_R \pi \Big/ \left[c(L + R_{di,dr})\right]$. The parameter $\Phi_{di,dr}$ are angle parameters given by $\Phi_{di,dr} = \left(2\sqrt{2}/\pi\right)\cos\left[\left(\phi_R \pm \phi_S\right)/2\right]$. Last the parameters τ_{lag}^{di} and τ_{lag}^{dr} are named diffraction time delay parameters and are defined as,

$$\tau_{lag}^{di,dr} = (\pi/2)t_{di,dr}\Phi_{di,dr}^2 = c^{-1}\left(L - R_{di,dr}\right), \tag{4}$$

where the distances R_{di} and R_{dr} are the direct distances from the source to the receiver and from the image-source of reflection to the receiver, respectively with $R_{di,dr} = \sqrt{r_S^2 + r_R^2 - 2r_R r_S\cos\left(\phi_S \mp \phi_R\right) + \left(z_S - z_R\right)^2}$. The parameters τ_{lag}^{di} and τ_{lag}^{dr} express the time difference between the arrival of the diffracted signals p_{irf}^{di} and p_{irf}^{dr}, and the arrival of the sound signals of incidence and reflection, respectively. τ_{lag}^{di} and τ_{lag}^{dr} are also measures of the angular distance of the receiver from the shadow boundaries SBI and SBR, respectively [Figure 1 (a)]. τ_{lag}^{di} decreases and approaches zero as the receiver moves closer to SBI. Same holds for τ_{lag}^{dr} as the receiver moves closer to SBR.

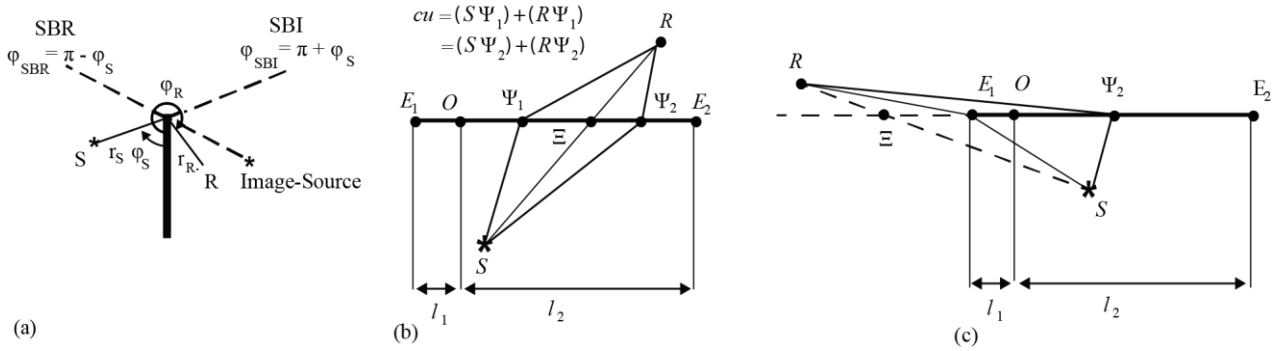

Figure 1 – Geometry of the finite edge side view (a), top view with reference point on the edge (b), top view with reference point outside the edge (c). Location of the reference point is $z_{\xi} = \left(z_R r_S + z_S r_R\right)/\left(r_S + r_R\right)$. u is the arrival time of the paths $S-\Psi_1-R$ and $S-\Psi_2-R$, respectively and c is the speed of sound.

3 Frequency Domain Solution

In this section a frequency domain diffraction solution for finite edges is going to be derived as the Fourier transform of the presented time domain impulse response solution. The Fourier transform of the time domain formula [Eq. (2)] is defined as,

$$\int_0^{\infty} e^{i\omega t}\, p^d_{irf,\,finite}(t)\, dt\,, \tag{5}$$

where ω is the angular frequency which is related to the ordinary frequency f as $\omega = 2\pi f$. For the study purposes the finite edge impulse response solution [Eq. (2)] is written in integral form,

$$p^d_{irf,\,finite} = \pm\frac{1}{2}\int_{L/c}^{L_1/c} \delta(t-u)\, p^d_{irf}(u)\, du + \frac{1}{2}\int_{L/c}^{L_2/c} \delta(t-u)\, p^d_{irf}(u)\, du\,, \tag{6}$$

where the integral variable u is defined in Figure 1 (b). Substituting Eq. (6) in Eq. (5) and also using Eq. (3) yields,

$$\begin{aligned} P^d_{\text{fin}} = \pm q_1^{di} + q_2^{di} \pm q_1^{dr} + q_2^{dr} = {} & \pm\frac{1}{2}\int_0^{\infty}\int_{L/c}^{L_1/c} e^{i\omega t}\delta(t-u)\, p^{di}_{irf}(u)\, du dt + \frac{1}{2}\int_0^{\infty}\int_{L/c}^{L_2/c} e^{i\omega t}\delta(t-u)\, p^{di}_{irf}(u)\, du dt \\ & \pm\frac{1}{2}\int_0^{\infty}\int_{L/c}^{L_1/c} e^{i\omega t}\delta(t-u)\, p^{dr}_{irf}(u)\, du dt + \frac{1}{2}\int_0^{\infty}\int_{L/c}^{L_2/c} e^{i\omega t}\delta(t-u)\, p^{dr}_{irf}(u)\, du dt. \end{aligned} \tag{7}$$

Equation (7) is a summation of four double integrals. Each integral is termed q_n^m, where the subscript n indicates the segment $\Xi E_1\left(n=1\right)$ or the edge segment $\Xi E_2\left(n=2\right)$ [Figure 1 (b) and (c)]. The superscript indicates the corresponding component of $p^d_{irf}(u)$ [Eq. (3)]. It is $m = di$ for $p^{di}_{irf}(u)$ and $m = dr$ for $p^{dr}_{irf}(u)$. It can be observed that the four integrals have similar form. In the following the integral q_1^{di} is going to be computed and the result will be similar for the rest integrals.

First, it is examined whether q_1^{di} is bounded. For that purpose, the Chaudhry and Zubair theorem [7] is used. According to this theorem q_1^{di} [Eq. (7)] is bounded if the integral $\int_{L/c}^{L_1/c}\int_0^{\infty}\left|e^{i\omega t}\delta(t-u)\, p^{di}_{irf}(u)\right| dt du$ is bounded. Indeed, the integral $\int_{L/c}^{L_1/c}\int_0^{\infty}\left|e^{i\omega t}\delta(t-u)\, p^{di}_{irf}(u)\right| dt du$ is equal to $\int_{L/c}^{L_1/c}\left|p^{di}_{irf}(u)\right| du$, which has been

proven to be bounded in previous work of the authors [5]. Furthermore, according to Chaudhry and Zubair theorem q_1^{di} not only is bounded but the order of integration can change without affecting the result. Thus, q_1^{di} can be written as

$$q_1^{di} = \frac{1}{2}\int_{L/c}^{L_1/c}\int_0^{\infty} e^{i\omega t}\delta(t-u)\, p_{irf}^{di}(u)\, dt du = \frac{1}{2}\int_{L/c}^{L_1/c} e^{i\omega u}\, p_{irf}^{di}(u)\, du\,, \tag{8}$$

The integral variable u is changed to $\tau = u - L/c$ for reasons of simplicity. Substituting $p_{irf}^{di}(u)$ from Eq. (3) in Eq. (8) and applying the variable change yields,

$$q_1^{di} = \int_0^{\tau_1} e^{i\omega\tau}\left(c^{di}/2\right)\left[\sqrt{\tau}\left(\tau+\tau_{lag}^{di}\right)\right]^{-1} d\tau,\; c^{di} = -\bar{t}_{di}\Phi_{di}e^{i\omega L/c}\sqrt{c}\Big/\left(2\pi\sqrt{L}\sqrt{r_S r_R}\right), \tag{9}$$

where c^{di} is the constant part of q_1^{di} with respect to τ. A parameter such as c^{di} will also appear in q_2^{di}. For q_1^{dr} and q_2^{dr} the counterpart of c^{di} will be $c^{dr} = -\bar{t}_{dr}\Phi_{dr}e^{i\omega L/c}\sqrt{c}\Big/\left(2\pi\sqrt{L}\sqrt{r_S r_R}\right)$. The integration in Eq. (9) is a summation of diffraction contributions coming from the segment ΞE_1. The integration variable τ represents the time difference between the arrival time u [Figure 1 (b)] of the reradiation path $S-\Psi_1-R$ [Figure 1 (b) and (c)] and the arrival time L/c [see Eq. (1)] of the reference path $S-\Xi-R$. Every value of τ in $[0,\tau_1]$ corresponds to one and only one edge point Ψ_1 on the edge segment ΞE_1. The lower limit $\tau = 0$ of the integral of Eq. (9) corresponds to $\Psi_1 \equiv \Xi$ and the upper limit $\tau = \tau_1 = L_1/c - L/c$ corresponds to $\Psi_1 \equiv E_1$.

For $\tau_1 \to \infty$ the integral q_1^{di} converges to its improper version which can be found in tables of integrals [8],

$$q_{1,\inf}^{di} = \int_0^{\infty}\frac{1}{2}c^{di}\frac{e^{i\omega\tau}}{\sqrt{\tau}\left(\tau+\tau_{lag}^{di}\right)}d\tau = \frac{1}{2}c^{di}\frac{\pi}{\sqrt{\tau_{lag}^{di}}}\times$$
$$\left\{\begin{array}{l}\cos\left(\omega\tau_{lag}^{di}\right)\left[1-C\left(\sqrt{\frac{2}{\pi}\omega\tau_{lag}^{di}}\right)-S\left(\sqrt{\frac{2}{\pi}\omega\tau_{lag}^{di}}\right)\right]+\sin\left(\omega\tau_{lag}^{di}\right)\left[C\left(\sqrt{\frac{2}{\pi}\omega\tau_{lag}^{di}}\right)-S\left(\sqrt{\frac{2}{\pi}\omega\tau_{lag}^{di}}\right)\right] \\ +i\cos\left(\omega\tau_{lag}^{di}\right)\left[C\left(\sqrt{\frac{2}{\pi}\omega\tau_{lag}^{di}}\right)-S\left(\sqrt{\frac{2}{\pi}\omega\tau_{lag}^{di}}\right)\right]-i\sin\left(\omega\tau_{lag}^{di}\right)\left[1-C\left(\sqrt{\frac{2}{\pi}\omega\tau_{lag}^{di}}\right)-S\left(\sqrt{\frac{2}{\pi}\omega\tau_{lag}^{di}}\right)\right]\end{array}\right\}, \tag{10}$$

where C is the cosine Fresnel integral and S is the sine Fresnel integral [9]. The components q_1^{di}, q_2^{di}, q_1^{dr}, and q_2^{dr} can be substituted for their improper counterparts $q_{1,\inf}^{di}$, $q_{2,\inf}^{di}$, $q_{1,\inf}^{dr}$, and $q_{2,\inf}^{dr}$ in Eq. (7) to yield the frequency diffraction formula for infinite edges [6]. To the best of the authors' knowledge the definite integral of Eq. (9) cannot be found either in existing tables or by using symbolic math software. An analytical calculation for q_1^{di} [Eq. (9)] is derived in the following.

To derive a solution for q_1^{di} its integrand function will be approximated by an analytical approximation whose integral is known. For $\tau_1 \le 10^{-8}$ the integrand function will be approximated as a whole in $[0,\tau_1]$, while for $\tau_1 > 10^{-8}$ a piecewise approximation will be used. For the piecewise approximation the interval of integration $[0,\tau_1]$ is separated to subintervals. The subintervals are: $[0,10^{-8}]..[10^{j-9},10^{j-8}]..[10^{k-9},\tau_1]$, $j = 0,1..k$ for $\tau_1 > 10^{-7}$ and $[0,10^{-8}],[10^{-8},\tau_1]$ for $\tau_1 \le 10^{-7}$. The total result for q_1^{di} is the integral of the analytical approximation for $\tau_1 \le 10^{-8}$, while for $\tau_1 > 10^{-8}$ it comes from the summation of the result of integration in each subinterval. The contribution of a subinterval to the total

result is termed $Q_{n,j}^{m}$, where the superscript is as in q_n^m, $m=di$ or $m=dr$. In the subscript of $Q_{n,j}^{m}$, the first digit "n" represents, as for q_n^m, the segment ΞE_1 (with *n=1*) or the segment ΞE_2 (*n=2*) of the edge [Figure 1 (b) and (c)] and the second digit represents the number of integration interval which is $j=0$ for $\left[0,10^{-8}\right]$, $j=1$ for $\left[10^{-8},10^{-7}\right]$ and so on.

For $\tau_1 \le 10^{-8}$ the Fourier term $e^{i\omega\tau}$ in Eq. (9) can be approximated as $e^{i\omega\tau} \simeq 1+\omega\tau$. This approximation is used up to $f=10^4\,\text{Hz}$. To maintain high accuracy for higher frequencies, the first segment would be $\left[0,10^{-9}\right]$ or smaller. For $\tau_1 > 10^{-8}$ the factor $1/\sqrt{\tau}$ in the subintervals $\left[0,10^{-8}\right]..\left[10^{j-9},10^{j-8}\right]..\left[10^{k-9},\tau_1\right]$ is approximated as,

$$1/\sqrt{\tau} \simeq \left(a_j e^{b_j\tau} + c_j e^{d_j\tau}\right)\Big/\sqrt{10^{j-9}} \qquad (11),$$

where the parameters a_j, b_j, c_j, d_j are least squares coefficients and their values for every subdomain are given in Table 1. The approximation of Eq. (11) yields very small error for every subdomain $\left[10^{j-9},10^{j-8}\right]$. For the case where the largest error occurs $(j=5)$ the least squares fitting yields $R^2=0.999$ and $RMSE=0.004$ which implies excellent accuracy.

Table 1. Coefficients of Eq. (11) and of Eq. (12).

j	a_j	b_j	c_j	d_j
1	0.886925464374122	-77610000	0.598457139494409	-6643300
2	0.896331776107598	-7761945.36818933	0.594803743968482	-654143.784748116
3	0.904712433836298	-778713.444368833	0.591159139220784	-64311.9038662154
4	0.878062270580339	-75524.7707578675	0.586271081481262	-6347.12255347972
5	0.876009124026327	-7358.69387190255	0.578883399646992	-621.592326306155
6	0.875573698167825	-735.152715751881	0.578631014255657	-62.1098100561987
7	0.875610800811663	-73.5226395039242	0.578656737686179	-6.21147099770718
8	0.875678813745594	-7.35314141360905	0.578686800205807	-0.621206386779095
9	0.875611245787398	-0.735244875671642	0.578666941955575	-0.0621166979493215

The approximation of Eq. (11) has been done up to $j=9$. That is because: (i) the integral q_1^{di} has converged to its infinite value $q_1^{di} \simeq 0.99 q_{1,\text{inf}}^{di}$ after $\tau_1=1, j=8$ for all frequencies up to $10^4\,\text{Hz}$, receiver and source locations. (ii) In practical problems, the reradiation time τ_1 does not exceed $10^{-4}\,\text{s}$ which corresponds to $j=4$.

Taking into account both approximations for $\tau_1 \le 10^{-8}$ and for $\tau_1 > 10^{-8}$ the total result for q_1^{di} is

$$q_1^{di} = \frac{1}{2} c^{di} \begin{cases} Q_{1,0}^{di} & , \tau_1 \le 10^{-8} \\ Q_{1,0}^{di}\big|_{10^{-8}} + \sum_{j=1}^{k} Q_{1,j}^{di} & , \tau_1 > 10^{-8} \end{cases}$$

$$Q_{1,0}^{di} = \frac{2}{\sqrt{\tau_{lag}^{di}}} \arctan\left(\sqrt{\frac{\tau_1}{\tau_{lag}^{di}}}\right) + \frac{2\omega i}{\sqrt{\tau_{lag}^{di}}}\left[\sqrt{\tau_1 \tau_{lag}^{di}} - \tau_{lag}^{di} \arctan\left(\sqrt{\frac{\tau_1}{\tau_{lag}^{di}}}\right)\right], \; x = \begin{cases} \tau_1 \text{ for } \tau_1 \le 10^{-8} \\ 10^{-8} \text{ for } \tau_1 > 10^{-8} \end{cases} \quad (12)$$

$$Q_{1,j}^{di} = \left.\begin{aligned} &-a_j N\left(x, \tau_{lag}^{di}, b_j, \omega\right) + a_j N\left(10^{j-9}, \tau_{lag}^{di}, b_j, \omega\right) \\ &-c_j N\left(x, \tau_{lag}^{di}, d_j, \omega\right) + c_j N\left(10^{j-9}, \tau_{lag}^{di}, d_j, \omega\right) \end{aligned}\right\}, \; x = \begin{cases} 10^{j-8} \text{ for } j < k \\ \tau_1 \text{ for } j = k \end{cases}$$

$$k = \left\{\begin{matrix} \text{floor}\left[\log_{10}(\tau_1)\right] + 9, \; \tau_1 \ne 10^{-8}, 10^{-7}..1 \\ \text{floor}\left[\log_{10}(\tau_1)\right] + 8, \; \tau_1 = 10^{-8}, 10^{-7}..1 \end{matrix}\right\} \text{floor}(x) \equiv \text{lowest integer close to } x$$

where a_j, b_j, c_j, d_j are coefficients that can be found in Table 1 and N is the following function,

$$N\left(x, \tau_{lag}^{di,dr}, 10^{j-9}, \omega\right) = e^{g-s} \mathrm{E}_{\text{int}}(g) = \begin{cases} e^{g-s} \mathrm{E}_1(g) & , |g| < 200 \\ \dfrac{e^{-s}}{g} & , |g| > 200 \end{cases} \quad (13)$$

$$g = -\left(x + \tau_{lag}^{di,dr}\right)\left(10^{j-9} + i\omega\right), \quad s = -x\left(10^{j-9} + i\omega\right)$$

where E_{int} is the exponential integral $\mathrm{E}_{\text{int}} = \int_1^\infty e^{-gt}/t \, dt$, of complex argument g [9]. The function "N" [Eq. (12)] expresses a multiplication of an exponential component (becomes very large in magnitude as the magnitude of g increases) and an exponential integral component (becomes very small in magnitude as the magnitude of g increases). For large $|g|$ the multiplication may be impossible to implement using existing hardware since it may require a very large number of digits. To deal with this issue the exponential integral is approximated by function N, for $|g| > 200$, with the first term of its asymptotic expansion, namely, $\mathrm{E}_{\text{int}} \simeq e^{-g}/g$ [9]. The multiplication becomes $e^{g-s}\mathrm{E}_{\text{int}}(g) = e^{g-s} \cdot e^{-g}/g = e^{-s}/g$ and can be easily calculated. The value 200 for the magnitude of g is so large that there is no loss in accuracy.

4 Accuracy of the frequency domain solution

The accuracy of the present solution is determined by comparisons with the well-established integral solution of Svensson et al. [3]. For the comparison purposes the following parameter is introduced,

$$error = 100\left(\left|P_{\text{fin}}^{d}\right| - |P_s|\right)\left(1/|P_s|\right), \quad (14)$$

where the symbol P_s is referred to the Svensson et al. solution [3]. Results for the *error* parameter of Eq. (14) are discussed for the case where the reference point lies on the edge or outside the edge [Figure 1 (b) and (c), respectively].

For both cases, the behavior of *error* has been studied with respect to the parameter kL, which expresses the length of the reference path normalized by the wavelength ($k = \omega/\mathrm{c} = 2\pi/\lambda$ is the wavenumber where λ is the wavelength), the parameters $c\tau_1/L$ and $c\tau_2/L$ (i.e. the arrival times of diffraction from the two edge ends normalized by the arrival time of the reference path L/c), and the parameters τ_{lag}^{di} and τ_{lag}^{dr} [Eq. (4)].

When the reference point lies on the edge [Figure 1 (b)], the error parameter has been found to be large for small values of kL, $kL<2$ (i.e., small frequencies or a source and a receiver located close to the edge). Furthermore, it has been observed that, from all receiver locations the largest values for error occur for $\tau_{lag}^{di}=\tau_{lag}^{dr}$ when the receiver is far from both shadow boundaries. For $kL=2$, $\tau_{lag}^{di}=\tau_{lag}^{dr}$, and $\tau_1=0$ $(E_1\equiv\Xi)$ the error increases as $c\tau_2/L$ increases (i.e. as the edge end E_2 moves far from the reference point Ξ). Similar results occur if both τ_1 and τ_2 are increased simultaneously $(\tau_1=\tau_2)$. The maximum error is 9.22%, occurs for small values of $c\tau_2/L$ and drops thereafter. For larger values of kL error drops. For $kL>7$ the error is less than 5%. For all values kL error drops as the receiver moves closer *SBI* or to *SBR* ($\tau_{lag}^{dr}\to 0$ or $\tau_{lag}^{di}\to 0$, respectively) being less than 5% for $kL=2$ and less than 2% for $kL=7$.

When the reference point is located outside the edge [Figure 1 (c)], E_1 lies on the right side of the reference point [Figure 1 (c)] and cannot move further from the location of E_2 $(\tau_1<\tau_2)$. Two cases for E_2 are considered (i) The case where E_2 moves to infinity and the edge becomes semi-infinite. In this case error is less than 10% for $kL\geq 7$ and $c\tau_1/L\leq 0.06$ and drops to 5% for $kL\geq 50$ and $c\tau_1/L\leq 0.06$. Error has been reported to grow very fast for all kL when τ_1 increases beyond $c\tau_1/L=0.06$. (ii) The case where the location of E_2 remains bounded. In this case error is less than 10% for $c\tau_2/L<0.1$ (i.e., when a finite edge is small compared to the source and the receiver radial distances r_S, r_R from the edge) irrespective of kL.

5 Convergence to the infinite edge solution

In this section, the convergence of the presented finite edge solution to the infinite edge solution as the length of the edge increases is investigated and proper limits after which one can handle the finite edge diffraction problem using the infinite edge solution are determined.

When the reference point is located on the edge [Figure 1 (b)], both edge ends E_1 and E_2 may extend to infinity ($l_1\to-\infty, l_2\to\infty$ and thus $\tau_1,\tau_2\to\infty$). In that case, as shown in section 3, the four integral components of P_{fin}^{d} namely, $q_1^{di}, q_2^{di}, q_1^{dr}, q_2^{dr}$ [Eq. (7)] converge to their infinite counterparts $q_{1,\text{inf}}^{di}, q_{2,\text{inf}}^{di}, q_{1,\text{inf}}^{dr}, q_{2,\text{inf}}^{dr}$ [Eq. (10)] and thus P_{fin}^{d} converges to P_{inf}^{d} (where P_{inf}^{d} stands for the infinite edge solution of ref. [6]). Let τ_{inf}^{d} be a critical value of τ_1 and τ_2 so that if $\tau_1,\tau_2\geq\tau_{\text{inf}}^{d}$, then P_{fin}^{d} is almost equal to P_{inf}^{d}. Also, let $\tau_{1,\text{inf}}^{di}$ be a critical value of q_1^{di} so that if $\tau_1\geq\tau_{1,\text{inf}}^{di}$, then q_1^{di} is almost equal to $q_{1,\text{inf}}^{di}$. Similar to $\tau_{1,\text{inf}}^{di}$, the critical values $\tau_{1,\text{inf}}^{dr}, \tau_{2,\text{inf}}^{di}, \tau_{2,\text{inf}}^{dr}$ are defined for $q_2^{di}, q_1^{dr}, q_2^{dr}$. For P_{fin}^{d} to be almost equal to P_{inf}^{d}, all integral components $q_1^{di}, q_2^{di}, q_1^{dr}, q_2^{dr}$ should be almost equal to $q_{1,\text{inf}}^{di}, q_{2,\text{inf}}^{di}, q_{1,\text{inf}}^{dr}, q_{2,\text{inf}}^{dr}$. Thus, the value τ_{inf}^{d} should be equal to the largest of $\tau_{1,\text{inf}}^{di}, \tau_{1,\text{inf}}^{dr}, \tau_{2,\text{inf}}^{di}$, and $\tau_{2,\text{inf}}^{dr}$. In the following, the calculation of the critical values $\tau_{1,\text{inf}}^{di}, \tau_{1,\text{inf}}^{dr}, \tau_{2,\text{inf}}^{di}$, and $\tau_{2,\text{inf}}^{dr}$ is shown.

The definition of $\tau_{1,\text{inf}}^{di}$ is expressed as,

$$\left|q_1^{di}-q_{1,\text{inf}}^{di}\right|\leq v\left|q_{1,\text{inf}}^{di}\right|,\ \text{for every}\ \tau_1\geq\tau_{1,\text{inf}}^{di}, \tag{15}$$

where v is an accuracy factor $(v\to 0)$. It is observed that the parameter $c^{di}/2$, which is independent of τ_1, is common in q_1^{di} and $q_{1,\text{inf}}^{di}$ [see Eqs. (9) and (10)] and can be dropped from Eq. (15). Thus, an equivalent definition of $\tau_{1,\text{inf}}^{di}$ is

$$\begin{aligned} &\left|q_1^{di}\right|_n - q_{1,\inf}^{di}\left|_n\right| \le v\left|q_{1,\inf}^{di}\right|_n\Big|, \text{ for every } \tau_1 \ge \tau_{1,\inf}^{di} \\ &q_1^{di}\left|_n = 2q_1^{di}/c^{di},\ q_{1,\inf}^{di}\right|_n = 2q_{1,\inf}^{di}/c^{di} \end{aligned}, \tag{16}$$

where $q_1^{di}\left|_n\right.$ and $q_{1,\inf}^{di}\left|_n\right.$ are the components q_1^{di} and $q_{1,\inf}^{di}$ normalized with their common factor $c^{di}/2$. The parameter $\tau_{1,\inf}^{di}$ can be calculated based on Eq. (16). As shown in Figure 2 (a), $\tau_{1,\inf}^{di}$ is the greatest value of τ_1 in the graph of $\left|q_1^{di} - q_{1,\inf}^{di}\right|$ for which $\left|q_1^{di}\right|_n - q_{1,\inf}^{di}\left|_n\right| = v\left|q_{1,\inf}^{di}\right|_n\Big|$. Both $q_1^{di}\left|_n\right.$ and $q_{1,\inf}^{di}\left|_n\right.$ are functions of two variables, the angular frequency ω and the diffraction time delay τ_{lag}^{di} [see Eq. (3)] and thus $\tau_{1,\inf}^{di}$ is also a function of these variables. Note here, that the dependence of $\tau_{1,\inf}^{di}$ on the source and receiver locations is described by τ_{lag}^{di} which is a function of all 6 coordinates of the source and the receiver [see Eq. (4)].

Numerical calculation of $\tau_{1,\inf}^{di}$ based on Eq. (16) has been carried out on a 100x100 grid of pairs $\left(f, \tau_{lag}^{di}\right)$ [for $v = 5\%$ in Eq. (16)] and the result is shown in Figure 3 (a). The frequency in Figure 3 (a) ranges from $f = 10\text{Hz}$ to $f = 10^4\,\text{Hz}$ and the diffraction time delay ranges from $\tau_{lag}^{di} = 10^{-8}\text{s}$ to $\tau_{lag}^{di} = 10^{-1}\text{s}$. The selected range for τ_{lag}^{di} corresponds to all the possible combination of source and receiver. The values of $\tau_{1,\inf}^{di}$ in Figure 3 (a) can be approximated with very good accuracy using least squares fitting. The result is the following equation:

$$\begin{aligned} &\tau_{1,\inf}^{di} = \exp\left(A_1 + A_5 \ln\left(\tau_{lag}^{di}\right)\ln(\omega) + A_4\left[\ln\left(\tau_{lag}^{di}\right)\right]^2 + A_5 \ln(\omega)\ln\left(\tau_{lag}^{di}\right) + A_6\left[\ln(\omega)\right]^2\right)\left(\tau_{lag}^{di}\right)^{A_2}(\omega)^{A_3} \\ &A_1 = 1.7526,\ A_2 = 0.5567,\ A_3 = -0.3949,\ A_4 = -0.0101,\ A_5 = -0.0213,\ A_6 = -0.0132,\ \text{for } v = 5\% \end{aligned} \tag{17}$$

The approximation of Eq. (17) is highly accurate yielding $R^2 = 0.9962$ and $RMSE = 0.1831$ and can be used to estimate $\tau_{1,\inf}^{di}$ without calculating q_1^{di}. Figure 3 (b) depicts the calculation of $\tau_{1,\inf}^{di}$ using Eq. (17) on the same grid of pairs $\left(f, \tau_{lag}^{di}\right)$ that has been used for Figure 3 (a). Good agreement is observed between the two figures.

The calculation of $\tau_{1,\inf}^{dr}, \tau_{2,\inf}^{di}, \tau_{2,\inf}^{dr}$ is similar to that of $\tau_{1,\inf}^{di}$. The critical value $\tau_{\inf}^{d}$ is found as the maximum of these values. Numerical investigation has shown that if $\tau_{lag}^{di} > \tau_{lag}^{dr}$, then $\max\left(\tau_{1,\inf}^{di}, \tau_{1,\inf}^{dr}\right) = \tau_{1,\inf}^{di}$.

When the reference point is located outside the edge [Figure 1 (c)], E_2 may move to infinity ($l_2 \to \infty$ and thus $\tau_2 \to \infty$) and the edge end E_1 may approach the location of the reference point Ξ ($l_1 \to z_\xi^+$ and thus $\tau_1 \to 0$). In this case, the components q_2^{di} and q_2^{dr} of P_{fin}^d converge to their infinite counterparts $q_{2,\text{inf}}^{di}$ and $q_{2,\text{inf}}^{dr}$ while the components q_1^{di} and q_1^{dr} go to zero. As a result, the finite edge solution P_{fin}^d converges to $P_{\text{inf}}^d/2$. In this case, in addition to τ_{inf}^d, another critical value needs to be determined. Let τ_{zero}^d be a critical value of τ_1 so that if $\tau_1 \le \tau_{\text{zero}}^d$ and $\tau_2 \ge \tau_{\text{inf}}^d$ then P_{fin}^d is almost equal to $P_{\text{inf}}^d/2$. Also, let $\tau_{1,\text{zero}}^{di}$ and $\tau_{1,\text{zero}}^{dr}$ be critical values of τ_1 so that if $\tau_1 \le \tau_{1,zero}^{di}$ and $\tau_1 \le \tau_{1,zero}^{dr}$, then q_1^{di} and q_1^{dr} are insignificant compared to $q_{1,\text{inf}}^{di}$ and $q_{1,\text{inf}}^{dr}$, respectively. For P_{fin}^d to be almost equal to $P_{\text{inf}}^d/2$, both q_1^{di} and q_1^{dr} should be insignificant and thus, τ_{zero}^d is chosen as the lesser between the critical values of $\tau_{1,\text{zero}}^{di}$ and $\tau_{1,\text{zero}}^{dr}$. In the following, the calculation of the critical values $\tau_{1,\text{zero}}^{di}$ and $\tau_{1,\text{zero}}^{dr}$ is shown.

The definition of $\tau_{1,\text{zero}}^{di}$ can be expressed as:

$$\left|q_1^{di} - q_{1,\text{inf}}^{di}\right| \le h\left|q_{1,\text{inf}}^{di}\right|, \text{ for every } \tau_1 \le \tau_{1,\text{zero}}^{di}, \tag{18}$$

where h is a real number that approaches unity ($h \to 1$). The normalization that has been applied to Eq. (16) can be also applied to Eq. (18) to yield,

$$\left|q_1^{di}\right|_n - q_{1,\text{inf}}^{di}\Big|_n\Big| \le h\left|q_{1,\text{inf}}^{di}\Big|_n\right|, \text{ for every } \tau_1 \le \tau_{1,\text{zero}}^{di}, \tag{19}$$

The parameter $\tau_{1,\text{zero}}^{di}$ can be found based on Eq. (19). As shown in Figure 2 (b), $\tau_{1,\text{zero}}^{di}$ is the lowest value of τ_1 in the graph of $\left|q_1^{di} - q_{1,\text{inf}}^{di}\right|$ for which $\left|q_1^{di}\right|_n - q_{1,\text{inf}}^{di}\Big|_n\Big| = h\left|q_{1,\text{inf}}^{di}\Big|_n\right|$. Similar to $\tau_{1,\text{inf}}^{di}$, $\tau_{1,\text{zero}}^{di}$ is a function of frequency and τ_{lag}^{di}. Numerical calculation of $\tau_{1,\text{zero}}^{di}$ based on Eq. (19) (for $h = 95\%$) has been done on the same 100x100 grid of $\left(f, \tau_{lag}^{di}\right)$. The result is shown in Figure 4 (a). Similar to $\tau_{1,\text{inf}}^{di}$, the values of $\tau_{1,\text{zero}}^{di}$ in Figure 4 (a) can be approximated with very good accuracy using least squares fitting. The result is the following equation:

$$\tau_{1,\text{zero}}^{di} = \exp\left(B_1 + B_5 \ln\left(\tau_{lag}^{di}\right)\ln(\omega) + B_4\left[\ln\left(\tau_{lag}^{di}\right)\right]^2 + B_5 \ln(\omega)\ln\left(\tau_{lag}^{di}\right) + B_6\left[\ln(\omega)\right]^2\right)\left(\tau_{lag}^{di}\right)^{B_2}(\omega)^{B_3} \tag{20}$$

$$B_1 = -6.8972,\ B_2 = 0.4596,\ B_3 = -0.6390,\ B_4 = -0.0370,\ B_5 = -0.0716,\ B_6 = -0.0303,\ \text{for } h = 95\%$$

The approximation of Eq. (20) yields very good accuracy ($R^2 = 0.9932$ and $RMSE = 0.2850$). Equation (20) can be used to estimate $\tau_{1,\text{zero}}^{di}$ without calculating the solution q_1^{di} for a given frequency f and τ_{lag}^{di}. Figure 4 (b) depicts the calculation of $\tau_{1,\text{zero}}^{di}$ using Eq. (17) on the same grid of pairs $\left(f, \tau_{lag}^{di}\right)$ that has been used for Figure 4 (a). Good agreement is observed between the two figures.

The calculation of $\tau_{1,\text{zero}}^{dr}$ is similar to that of $\tau_{1,\text{zero}}^{di}$. The critical value τ_{zero}^{d} is found as the minimum between these values. Numerical investigation has shown if $\tau_{lag}^{di} > \tau_{lag}^{dr}$, then $\min\left(\tau_{1,\text{zero}}^{di}, \tau_{1,\text{zero}}^{dr}\right) = \tau_{1,\text{zero}}^{dr}$.

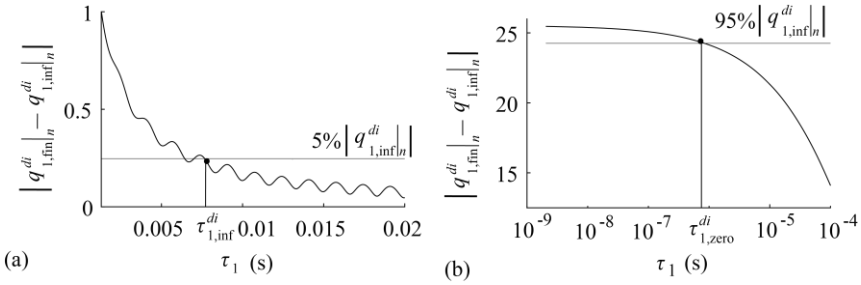

Figure 2 – Graphical example of Eq. (16) (a) and of (19) (b) for $v = 5\%$ and $h = 95\%$, respectively.

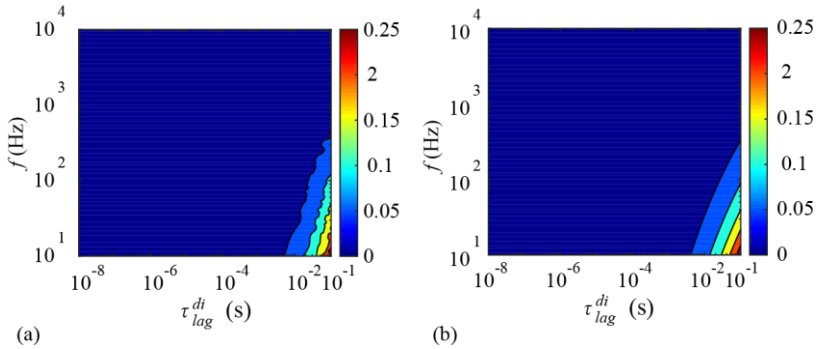

Figure 3 – Contours of $\tau_{1,\text{inf}}^{di}$ calculated numerically by solving the equality in Eq. (16) as shown in Figure 2 (a) and directly by Eq. (17) (b).

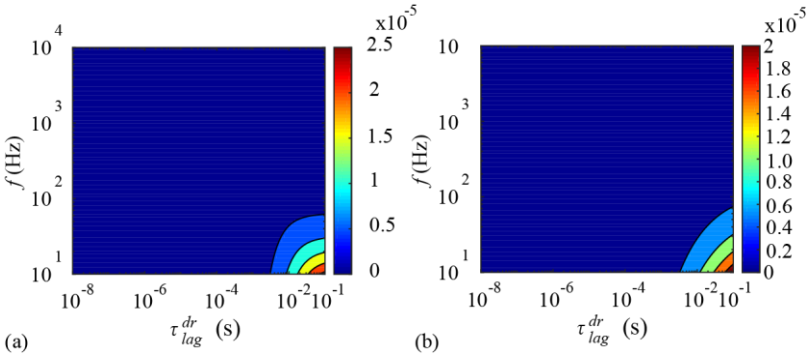

Figure 4 – Contours of $\tau^{di}_{1,\text{zero}}$ calculated numerically by solving the equality in Eq. (19) as shown in Figure 2 (b) and directly by Eq. (20) (b).

6 Conclusions

In the present work a frequency domain solution for the diffraction of spherical waves by finite edges has been derived. The presented solution has been derived as the Fourier transform of a time domain impulse response solution [5] and its accuracy has been determined by comparisons with the well-established Svensson et al. formula [3]. Finally, based on the presented solution, specific limits have been determined after which the diffraction solution for the infinite edge can be used to a finite edge diffraction problem.

References

[1] Kirchhoff, G. *Gesammelte Abhandlungen : Nachtrag*, (in German), Johann Ambrosius Barth, Leipzig (Germany), 1891.

[2] Menounou, P.; Papaefthymiou, E. S. Shadowing of directional noise sources by finite noise barriers, *Applied acoustics*, Vol 71(4), 2008, pp 351-367.

[3] Svensson, U. P.; Calamia, P. T.; Nakanishi, S. Frequency-domain edge diffraction for finite and infinite edges, *Acta Acustica united with Acustica*, Vol 95(3), 2009, pp 568-572.

[4] Ufimtsev, P. Ya. *Fundamentals of the Physical Theory of Diffraction*, John Wiley and Sons, Inc., Hoboken (USA), Second Edition, 2014.

[5] Nikolaou, P.; Menounou, P. Analytical and numerical methods for efficient calculation of edge diffraction by an arbitrary incident signal. *Journal of Acoustical society of America*, Vol 146(5), 2019, pp 3577-3589.

[6] Menounou, P.; Nikolaou, P. An extension to the directive line source model for diffraction by half-planes and wedges. *Acta Acustica united with Acustica*, Vol 102, 2016, pp 307–321.

[7] Chaudhry, M. A.; Zubair, M. S. *On a Class of Incomplete Gamma Functions with Applications*, CRC Press, Boca Raton, Florida (USA), 2001.

[8] Oberhettinger, F. *Tables of Fourier transforms and Fourier transforms of distributions*, Springer Science & Business Media, Berlin/Heidelberg (Germany), 2012.

[9] Abramowitz, M.; Stegun, I. A. *Handbook of Mathematical Functions with Formulas, Graphs, and Mathematical Tables*. Dover Publications, NY (USA), 1972.